

PCCP

Accepted Manuscript



This is an *Accepted Manuscript*, which has been through the Royal Society of Chemistry peer review process and has been accepted for publication.

Accepted Manuscripts are published online shortly after acceptance, before technical editing, formatting and proof reading. Using this free service, authors can make their results available to the community, in citable form, before we publish the edited article. We will replace this *Accepted Manuscript* with the edited and formatted *Advance Article* as soon as it is available.

You can find more information about *Accepted Manuscripts* in the [Information for Authors](#).

Please note that technical editing may introduce minor changes to the text and/or graphics, which may alter content. The journal's standard [Terms & Conditions](#) and the [Ethical guidelines](#) still apply. In no event shall the Royal Society of Chemistry be held responsible for any errors or omissions in this *Accepted Manuscript* or any consequences arising from the use of any information it contains.



Physical Chemistry Chemical Physics

ARTICLE

Liquid-Liquid Equilibria of Binary Mixtures of a Lipidic Ionic Liquid with Hydrocarbons

B. D. Green,^a A. J. Badini,^a R. A. O'Brien,^b J. H. Davis, Jr.,^b and Kevin N. West^{a,*}Received 00th January 20xx,
Accepted 00th January 20xx

DOI: 10.1039/x0xx00000x

www.rsc.org/

Although structurally diverse, many ionic liquids (ILs) are polar in nature due to the strong coulombic forces inherent in ionic compounds. However, the overall polarity of the IL can be tuned by incorporating significant nonpolar content into one or more of the constituent ions. In this work, the binary liquid-liquid equilibria of one such IL, 1-methyl-3-(Z-octadec-9-enyl)imidazolium bistriflimide, with several hydrocarbons (*n*-hexane, *n*-octane, *n*-decane, cyclohexane, methylcyclohexane, 1-octene) is measured over the temperature range 0-70°C at ambient pressure using a combination of cloud point and gravimetric techniques. The phase behavior of the systems are similar in that they exhibit two phases: one that is 60-90 mole % hydrocarbon and a second phase that is nearly pure hydrocarbon. Each phase exhibits a weak dependence of composition on temperature (steep curve) above ~10°C, likely due to swelling and restructuring of the nonpolar nano-domains of the IL being limited by energetically unfavorable restructuring in the polar nano-domains. The solubility of the *n*-alkanes decreases with increasing size (molar volume), a trend that continues for the cyclic alkanes, for which upper critical solution temperatures are observed below 70°C. 1-Octene is found to be more soluble than *n*-octane, attributable to a combination of its lower molar volume and slightly higher polarity. The COSMO-RS model is used to predict the T-x-x' diagrams and gives good qualitative agreement of the observed trends. This work presents the highest known solubility of *n*-alkanes in an IL to date and tuning the structure of the ionic liquid to maximize the size/shape trends observed may provide the basis for enhanced separations of nonpolar species.

1. Introduction

Ionic liquids (ILs) are a broad class of salts with a variety of different chemical structures and thermophysical properties, unified in that they are composed solely of ions and have melting points lower than 100°C. As many examples of these compounds are also liquids at or near room temperature, there has been great interest from academia and from industry in investigating their potential as replacement solvents for volatile organic compounds used in the chemical process industry.^{1, 2} Being composed of ions, many ionic liquids have vanishingly low vapor pressures, which significantly reduces the possibility that they will contribute to fugitive emissions when used as solvents. Additionally, their physical and chemical properties may be tuned by altering the chemical structures present in the cation and in the anion, resulting in an abundance of potential pairs with which to form new ionic liquids.^{3, 4}

To date, ionic liquids have been investigated for use as solvents for many processes including gas separations,⁵⁻¹⁰ liquid-liquid extractions¹¹⁻¹⁷ and numerous classes of reactions.¹⁸⁻²⁴ For the vast majority of ionic liquids, the ionic nature of the species and

often dominant coulombic forces yield liquids with polar to moderately polar solvent strength, as evidenced by their high solubility for more polar solutes, including polar and moderately polar liquids and salts.^{11, 25, 26} However, a descriptor of the overall polarity of traditional ionic liquids is somewhat elusive, in that when solvatochromic dyes are used to probe the solvent environment, the results indicate a more polar medium than when a technique such as dielectric spectroscopy is used.^{27, 28} The divergence in these measurements is likely due to the bulk/continuum nature of dielectric spectroscopy as opposed to the highly localized solvent environment reported by dyes. Thus, if the dye partitions to a more polar region, a more polar environment will be observed. This is to be expected given the heterogeneous nanostructure of ionic liquids, well described in a recent review²⁹ and considered below.

Furthermore, it has been effectively demonstrated that traditional ionic liquids have low solubilities in alkanes and cycloalkanes and higher solubilities in aromatic hydrocarbons.^{30, 31} Interestingly, this is similar to the binary behavior of ionic liquids with CO₂, in that CO₂ has a high solubility in many traditional ionic liquids³² (relative to other nonpolar solutes³³) while ionic liquids are virtually insoluble in CO₂.³⁴ Recently, several research groups have focused on developing ionic liquids with significant nonpolar solvent character by incorporating substantial nonpolar content into the structure of the ionic liquid. Liu *et al.*³⁵⁻³⁸ have demonstrated the ability of tetraalkylphosphonium phosphinates to solubilize small hydrocarbon gases better than conventional, more polar ionic

^a Department of Chemical & Biomolecular Engineering, University of South Alabama, Mobile, AL 36688 (USA).

^b Department of Chemistry, University of South Alabama, Mobile, AL 36688 (USA).

*Corresponding Author: Dr. Kevin N. West, Associate Professor, Department of Chemical & Biomolecular Engineering, University of South Alabama, Mobile, AL 36688, kevinwest@southalabama.edu, 251.460.7563

liquids. In a similar fashion, our research group has developed a class of ionic liquids which we call lipidic ionic liquids, as they were inspired by and are synthesized from naturally occurring lipids.³⁹⁻⁴² This class of ionic liquids is comprised of 1-alkyl-3-methylimidazolium bistriflimides where the alkyl chain contains 16 or more carbons.

Like natural lipids, 1-alkyl-3-methylimidazolium-based ionic liquids with long saturated alkyl chains (greater than ~9 carbon atoms) tend to have melting points that increase with chain length as a result of increased dispersion forces.⁴³⁻⁴⁷ For a variety of compounds, this results in room temperature solids. However, we have shown that, like natural lipids, incorporating an unsaturation (double bond) near the midpoint of the alkyl chain significantly reduces the melting point.⁴¹ *Cis* oriented double bonds, which introduce a “kink” into the chain, have a more pronounced effect than do *trans* oriented bonds. When a *cis* unsaturation is placed at the 9-10 position in a C₁₈ alkyl side chain, the melting point is reduced by more than 70°C relative to the saturated C₁₈ chain. Similar effects are observed when the double bond is replaced with other symmetry breaking moieties such as cyclopropyl groups⁴⁸ or sulfur atoms.⁴⁹ Compounds resulting from the latter modification, synthesized through the use of thiol-ene “click chemistry,”⁵⁰ exhibited melting points with a strong dependence on the position of the sulfur atom in the alkyl side chain.

Recently, we have investigated the solubility of ethane and ethylene in the representative lipidic ionic liquid mentioned above, 1-(*Z*-octadec-9-enyl)-3-methylimidazolium bistriflimide (**Figure 1**), which contains an 18 carbon side chain with a *cis* double bond in the 9-10 position.⁵¹ This side chain is akin to the *cis* unsaturated fatty acid from which it is derived, oleic acid, and as such we abbreviate this ionic liquid as [oleyl-mim][NTf₂]. Similar to the behavior Liu *et al.* described for the tetraalkyl phosphinates,³⁸ we observed high solubilities for both ethylene and ethane, with ethane having a higher solubility in the IL. This is in contrast to most conventional ionic liquids which show higher ethylene solubility, a result of the interaction of the π bond on ethylene with the polar/aromatic regions of the ionic liquid. Higher ethane solubility in ionic liquids with substantial nonpolar content indicates that the additional nonpolar structural components are effectively increasing the lipophilicity of the ionic liquids, resulting in ionic liquids with more “nonpolar-like” solvent properties.

To further characterize the solvent properties of these ionic liquids, we now turn our attention to describing the liquid-liquid

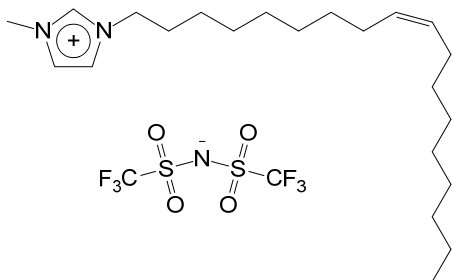


Figure 1 – Structure of the lipidic ionic 1-methyl-3-(*Z*-octadec-9-enyl)imidazolium bistriflimide ([oleyl-mim][NTf₂]).

equilibria (LLE) of [oleyl-mim][NTf₂] with a number of molecular liquids, primarily *n*-alkanes and cycloalkanes, using a combination of cloud point and gravimetric techniques. There is a growing literature describing LLE and infinite dilution activity coefficients of ionic liquids with nonpolar solutes.^{25, 26, 52-55} Additionally, there is considerable literature investigating ternary systems of aromatics, aliphatics and ionic liquids focused on separating aromatics from aliphatics by extracting them into an ionic liquid.^{15, 56-60}

In general, for binary alkane-IL systems, it is observed that as the size of the *n*-alkane increases, alkane solubility in the ionic liquid decreases, with cyclic alkanes having higher solubility than similarly-sized *n*-alkanes due to the smaller molar volume of analogous cyclic alkanes. Additionally, for a fixed *n*-alkane, solubility in the ionic liquid increases as the alkyl side chain on the imidazolium-based ionic liquid increases. Similarly, alkane infinite dilution activity coefficients increase with increasing *n*-alkane size for a given ionic liquid and decrease for a fixed *n*-alkane as the length of the alkyl side chain on the ionic liquid increases.^{25, 26, 52, 53} These trends, along with molecular dynamic simulations, support the picture of these ionic liquids having a heterogeneous nanostructure, with aggregation of the alkyl tails producing nonpolar domains and clustering of polar/ionic regions producing polar domains.⁶¹⁻⁶⁵ Such a nanostructure would be limited in the size/amount of nonpolar solute that would fit into the nonpolar domain, resulting in the trends observed for both alkane and IL alkyl side chain size. Accommodation of additional solute would involve restructuring the polar/ionic regions which would have a higher energy penalty.

Through molecular dynamic simulation, Wang and Vooth showed that ionic liquids exhibit spatial heterogeneity at the nano-scale.⁶⁴ Additionally, Lopes and Padua⁶¹ demonstrated that as the size of the side chain increases from C₂ to C₆, the nanostructure of the ionic liquid changes from one of continuous polar regions with “islands” of nonpolar tails to one of continuous nonpolar regions. With such a transition happening for a 1-alkyl-3-methylimidazolium-based ionic liquids at a chain length of 6 carbons, the nanostructure of [oleyl-mim][NTf₂] with a C₁₈ side chain is likely to be controlled by the interaction of the alkyl chains, providing a significant micro-volume available for the solvation of nonpolar species.

More recently, molecular dynamic simulations have expanded this analysis to more fully characterize the structure of 1-alkyl-3-methylimidazolium-based ionic liquids at the nanoscale, and how this structure evolves as the size of the alkyl side chain is increased. Shimizu *et al.* performed a comprehensive molecular dynamics study of the bistriflimide salts of this class of ionic liquids with alkyl chains ranging from C₂-C₁₀.⁶⁶ The results agreed with previous studies which indicated that a continuous nonpolar domain develops as the side chain is increased above C₆, and also that the polar domain remains continuous as well. Interestingly, the researchers also found that as the nonpolar domain becomes continuous, the polar domain is “partially broken (although without losing its three-dimensional continuity) in order to accommodate progressively larger nonpolar domains” and they described this partial breaking of

the domain as “swelling”. In another study which introduced new method for analyzing the results of molecular dynamic simulation, the continuity of the nonpolar domain was also affirmed, although the scope of this work included a larger variety of shorter side chains (alkyl vs. fluorinated) and anions.⁶⁷ These previous investigations point towards increasing alkane solubility with increased alkyl side chain length for imidazolium-based ionic liquids, with potential solubility limitations based on polar domain restructuring. However, due to the increasing melting point trends mentioned above, it was not possible to extend phase behavior studies to longer chain ionic liquids as they were no longer liquids at the desired conditions. With the low melting lipidic ionic liquids described by our group, it is now possible to investigate the multicomponent phase equilibria of longer chain ionic liquids. In this work we demonstrate the continuation of the solubility trends previously observed using [oleyl-mim][NTf₂] as a representative lipidic ionic liquid, significant enhancements in hydrocarbon solubility and the highest yet reported solubility of alkanes in ionic liquids. Additionally, like many of the conventional ionic liquids, the solubility of the IL in the alkane phase is extremely low, indicating that little ionic liquid would be stripped into a nonpolar molecular phase and lost in extraction processes.

2. Experimental & Computational Methods

2.1. Materials

n-Hexane (99+%), *n*-octane (99+%), *n*-decane (99+%), 1-octene (99+%), cyclohexane (99.5%) and methylcyclohexane (99+%) were obtained from Acros Organics and used with further purification, save contacting with molecular sieves for ~ 2 hours prior to use.

2.2. Materials

The ionic liquid, [oleyl-mim][NTf₂], was synthesized by methods previously described and verified to have ≥99% purity via NMR.^{41, 68} Samples were placed in a rotary evaporator (~2 mbar, 40-60°C) for at least 24 hours in the prior to measurement.

2.3. Cloud Point Measurements

LLE was measured by cloud point and gravimetric techniques for binary mixtures containing the ILs and the molecular compounds, which were chosen to be non-polar and varying in size and shape to probe the ability of the ILs to solvate non-polar solutes. Mixtures were made of known mole fractions of [oleyl-mim][NTf₂] and the following compounds: *n*-hexane, *n*-octane, 1-octene, *n*-decane, cyclohexane, and methylcyclohexane. Binary samples were prepared in ~10 mL quantities using 1-15 g of each component measured on a balance with a precision of ±0.00001 g, resulting in mole fractions of a precision of ±0.0001. The samples were transferred to a sealed jacketed view cell where cooling/heating fluid was circulated in the jacket. The temperature of the liquid was measured directly using a K-type thermocouple and display with NIST traceable calibration to a precision of 0.1 K. The temperature of the mixture was raised to achieve a clear, homogenous solution and then the

temperature was lowered slowly to yield a non-homogeneous, cloudy solution. The temperature at which the solution changes from homogeneous to heterogeneous (cloudy) marks the solubility limit of the mixture and is recorded as the cloud point temperature. This process was repeated 3 times for reproducibility to achieve an uncertainty in temperature of +/- 1°C for slightly volatile compounds (*n*-octane, *n*-decane, cyclohexane, methylcyclohexane, 1-octene) and +/- 2°C for more volatile compounds (*n*-hexane) which had more variability due to slight vaporization of the molecular component in the headspace of the cell.

2.4. Gravimetric Measurements

For the gravimetric method, a sufficient quantity of each component (IL and hydrocarbon) was added to the cell described above to form two phases of ~5-8 mL each. The heterogeneous mixture was stirred and heated at a given temperature (±0.1 °C) for 1 hour, after which mixing was halted and the mixture was allowed to phase separate. Triplicate samples from the top and bottom phases were taken after 30 minutes weighed in pre-massed (±0.00001 g) vials, and were then left to dry in an oven (~50°C) for 24 hours, allowing the hydrocarbon component to vaporize, leaving the ionic liquid. The vials were then weighed and the mole fractions of each component were calculated. The values shown are the average of the three samples with the uncertainty given as the standard deviation of the mean, with a limiting minimum value of ±0.0001 based on the purity of the ionic liquid. For initial runs, the mixtures were allowed to phase separate for 30 minutes, 1 hour and 2 hours; however, it was observed that the mole fractions of each phase did not vary greater than the precision of the measurement as the phase separation time increased from 30 minutes to 2 hours. This was done for various temperatures to develop both sides of the T-x'-x'' diagram descriptive of the phase behavior.

2.5. COSMO-RS Modelling

Experimental LLE data are compared with those calculated by the COSMO-RS method⁶⁹ as implemented in COSMOthermX²⁰ version C30-1401 using BP-TZVP-C30-1401 parameterization. The ionic liquid was treated as independent ions with equal mole fractions. The database of compounds provided in the software (BP-TZVP-COSMO) included *n*-hexane, *n*-octane, *n*-decane, cyclohexane, methylcyclohexane and the bistriflimide anion, the latter being represented by two conformers. For 1-butene and the cation ([oleyl-mim]⁺) TURBOMOLE version 6.629²¹ was used to generate the COSMO-RS input files at the BVP-86/TZVP/DGA1 computational level, which is the standard method in the software and has been used by a number of investigators applying COSMO-RS to systems involving ionic liquids. COSMOconfX version 3.032²² was used to search for multiple conformer contributions with three found to be significant for the ionic liquid and two for 1-octene. The multiple conformer method in COSMOthermX was used for both ions and several of the molecular compounds. The LLE miscibility gap mole fractions as a function of temperature are

reported as the values calculated for the binodal LLE curve using the “laboratory-binary” framework, with the cation/anion pair treated as a single species when calculating mole fractions, consistent with experimental measurements.

3. Results & Discussion

3.1. Liquid-Liquid Equilibria

The data for both the cloud point and the gravimetric experiments are shown in **Tables 1-6** for *n*-hexane, *n*-octane, *n*-decane, cyclohexane, methylcyclohexane and 1-octene, respectively. These results are also shown graphically in **Figure 2**. For each binary pair, the same overall phase behaviour is observed: the presence of one phase which is 60-90% alkane, with the balance being ionic liquid, and a second phase that is nearly pure alkane, thus demonstrating that the ionic liquid has a high solubility for the nonpolar hydrocarbon, while remaining nearly insoluble in the hydrocarbon phase.

Additionally, several trends appear in the data with respect to the solubility of the hydrocarbon in the alkane as a function of its size, shape and saturation level. First, among the linear alkanes, as the size (molar volume) of the alkane increases from *n*-hexane to *n*-octane to *n*-decane, the solubility in the ionic liquid decreases. In addition to this trend, there is a steep vertical portion of the curve corresponding to a maximum alkane solubility that is relatively independent of temperature. Both of these observations can be explained by the nano-phase structure of the ionic liquid being segregated into polar and nonpolar domains. Within the nonpolar domains, there is a limited volume to solvate the nonpolar species, thus more of the smaller *n*-hexane molecules are soluble than are the larger *n*-decane molecules. Furthermore, as the alkane is dissolved into the polar domain, the domain likely expands, restructuring the ionic liquid to some degree, to accommodate the dissolved species. However, at some degree of expansion, the restructuring will begin to significantly disrupt the polar region of the liquid, an endothermic process which will require higher temperature, thus the steep “wall” observed on all of the plots. The *n*-alkanes also exhibit a lower slope region at lower temperatures that may be attributable to gelling effects, commonly observed with this class of ionic liquids at sub-ambient conditions.

With the cycloalkanes, upper critical solution temperatures were observed, although they would likely have been observed for the *n*-alkanes as well at higher temperatures than allowed by the experimental apparatus. In addition to observing the upper critical solution temperatures, the cycloalkanes were more soluble than their *n*-alkane analogues, with cyclohexane being slightly more soluble than methylcyclohexane. As will the *n*-alkanes, the solubility trend follows that of molar volume, with smaller species having higher solubilities.

Lastly, the phase behaviour of 1-octene with the ionic liquid was measured to examine the effect of including an unsaturation in the molecule, which increases its polarity slightly. 1-Octene exhibited slightly higher solubility in the ionic liquid than its saturated analogue, *n*-octane. While 1-octene does have a marginally smaller molar volume than 1-octene (158 cm³/mol

vs. 164 cm³/mol at 25°C),⁷³ the cause of its increased solubility may be the ability of its π electrons to interact with the polar domain of the ionic liquid. Specifically, it has recently been demonstrated that solutes, such as CO₂, may have significant interactions with π electrons of aromatic cations in ionic liquids.⁷⁴ Like CO₂, the terminal unsaturation in 1-octene could be experiencing an attractive interaction with the aromatic region of the cation as observed in these *ab initio* molecular dynamics studies, leading to enhanced solubility over its saturated analogue. The trends of increasing solubility with decreasing molar volume can be clearly seen in **Figure 3** which plots the solubility of each hydrocarbon at 25°C in the ionic liquids vs. the molar volume of the hydrocarbon.

Additional insights are obtained by comparing the solubility of *n*-hexane at 25°C in the lipidic ionic liquid and in shorter chain 1-alkyl-3-methylimidazolium bistriflimides.⁷⁵ The solubility trend as a function of the alkyl chain length on the ionic liquid, shown in **Figure 4**, is remarkably linear with the unsaturated 18 carbon chain species ([oleyl-mim][NTf₂]) exhibiting behaviour quite close to that predicted by the aforementioned linear trend for the saturated species. This indicates that the lipidic ionic liquid has solvent properties similar to what would be expected for the saturated C₁₈ appended imidazolium bistriflimide; however, such a measurement at 20°C isn't possible, as the saturated C₁₈ species melts at 53.5°C.⁴¹ We note that the lipidic ionic liquid was found to be miscible with methanol, ethanol, isopropanol, acetone and toluene over the temperature range examined.

The behaviour described above is similar to that of shorter chain 1-alkyl-3-methylimidazolium-based ionic liquids (methylsulfates) with aromatics such as benzene and toluene,¹³ where low solubilities of the ionic liquid are observed or predicted in the hydrocarbon phase while high solubilities of the hydrocarbon, with the characteristic steep wall, are observed for the ionic liquid. Of note is that although the behaviour is similar to that presented here, this was observed for aromatic/ionic liquid systems and aliphatic solubilities for the ionic liquids in the previous studies were still quite low.

The results of these binary systems can be further understood by comparing them to recent pure component molecular dynamics studies describing the evolution of nano-scale structures as the alkyl chain length of a 1-alkyl-3-methylimidazolium is increased. In the work presented here, nonpolar molecular species are being added to the nonpolar domain in the nano-heterogeneous ionic liquid; in the molecular dynamics study,⁶⁶ the bonded nonpolar appendage is being enlarged. In both cases the nanostructure of ionic liquid is being altered to accommodate additional nonpolar moieties. Shimizu *et al.*⁶⁶ found that as the alkyl chain length was increased, and a continuous nonpolar sub-phase/domain emerged (above a chain size of C₆), the polar domain remained continuous, although it was distorted to accommodate the additional nonpolar material. This is very similar to adding nonpolar material, in the form of hydrocarbons, to the pure component, and analogous distortion of the continuous polar phase would be expected. However, in the case of adding a hydrocarbon to the ionic liquid, there would likely be a limit to

Physical Chemistry Chemical Physics

ARTICLE

Table 1 – Cloud point and gravimetric liquid/liquid equilibria data for (1) *n*-hexane / (2) [oleyl-mim][NTf₂].

Cloud Point		<u><i>n</i>-Hexane</u>		Gravimetric		
<i>T</i> / °C (±2°C)	<i>x</i> ₁ (±0.0001)	<i>T</i> / °C (±0.1°C)	<i>x</i> ₁ [']	<i>u</i> _c ['] (±)	<i>x</i> ₁ ^{''}	<i>u</i> _c ^{''} (±)
-3.0	0.5940	0.0			0.9997	0.0002
1.0	0.7217	10.0	0.8368	0.0001	0.9997	0.0001
1.5	0.7609	20.0	0.8199	0.0001	1.0000	0.0001
2.0	0.7999	30.0	0.8152	0.0001	0.9957	0.0001
2.5	0.8292	40.0	0.8116	0.0001	1.0000	0.0001
50.0	0.8353	50.0	0.8198	0.0001	0.9998	0.0001

Table 2 – Cloud point and gravimetric liquid/liquid equilibria data for (1) *n*-octane / (2) [oleyl-mim][NTf₂].

Cloud Point		<u><i>n</i>-Octane</u>		Gravimetric		
<i>T</i> / °C (±1°C)	<i>x</i> ₁ (±0.0001)	<i>T</i> / °C (±0.1°C)	<i>x</i> ₁ [']	<i>u</i> _c ['] (±)	<i>x</i> ₁ ^{''}	<i>u</i> _c ^{''} (±)
-1.5	0.5002	10.0	0.7748	0.0001	0.9938	0.0008
3.0	0.6002	20.0	0.7750	0.0002	0.9998	0.0001
3.0	0.6022	30.0	0.7647	0.0001	0.9995	0.0001
6.5	0.6953	40.0	0.7567	0.0001	0.9997	0.0001
6.5	0.7395	50.0	0.7520	0.0001	0.9960	0.0001
7.0	0.7472					
6.0	0.7508					

Table 3 – Cloud point and gravimetric liquid/liquid equilibria data for (1) *n*-decane / (2) [oleyl-mim][NTf₂].

Cloud Point		<u><i>n</i>-Decane</u>		Gravimetric		
<i>T</i> / °C (±1°C)	<i>x</i> ₁ (±0.0001)	<i>T</i> / °C (±0.1°C)	<i>x</i> ₁ [']	<i>u</i> _c ['] (±)	<i>x</i> ₁ ^{''}	<i>u</i> _c ^{''} (±)
5.0	0.6002	10.0			0.9981	0.0001
5.0	0.6220	20.0	0.6515	0.0003	0.9972	0.0001
6.0	0.6407	30.0	0.6314	0.0006	0.9981	0.0001
		40.0	0.6319	0.0002	0.9977	0.0001
		50.0	0.6258	0.0004	0.9966	0.0001
		60.0	0.6303	0.0002	0.9982	0.0001

Table 4 – Cloud point and gravimetric liquid/liquid equilibria data for (1) cyclohexane / (2) [oleyl-mim] [NTf₂].

Cloud Point		<u>Cyclohexane</u>		Gravimetric		
$T/^\circ\text{C}$ ($\pm 1^\circ\text{C}$)	x_1 (± 0.0001)	$T/^\circ\text{C}$ ($\pm 0.1^\circ\text{C}$)	x_1'	u'_c (\pm)	x_1''	u''_c (\pm)
-1.5	0.7997	10.0	0.8963	0.0001	0.9995	0.0001
1.0	0.8698	30.0	0.9158	0.0001	0.9992	0.0001
16.5	0.9016	50.0	0.9168	0.0001	0.9983	0.0001
35.0	0.9212					
56.5	0.9502					

Table 5 – Cloud point and gravimetric liquid/liquid equilibria data for (1) methylcyclohexane / (2) [oleyl-mim] [NTf₂].

Cloud Point		<u>Methylcyclohexane</u>		Gravimetric		
$T/^\circ\text{C}$ ($\pm 1^\circ\text{C}$)	x_1 (± 0.0001)	$T/^\circ\text{C}$ ($\pm 0.1^\circ\text{C}$)	x_1'	u'_c (\pm)	x_1''	u''_c (\pm)
12.5	0.8860	0.0	0.8876	0.0001	1.0000	0.0001
33.0	0.9003	20.0	0.8973	0.0001	0.9998	0.0001
49.0	0.9202	40.0	0.9136	0.0001	0.9991	0.0001
53.0	0.9299					
58.0	0.9400					
61.0	0.9500					
63.5	0.9800					
64.0	0.9700					

Table 6 – Cloud point and gravimetric liquid/liquid equilibria data for (1) 1-octene / (2) [oleyl-mim] [NTf₂].

Cloud Point		<u>1-Octene</u>		Gravimetric		
$T/^\circ\text{C}$ ($\pm 1^\circ\text{C}$)	x_1 (± 0.0001)	$T/^\circ\text{C}$ ($\pm 0.1^\circ\text{C}$)	x_1'	u'_c (\pm)	x_1''	u''_c (\pm)
18.0	0.8311	10.0	0.8269	0.0001	0.9992	0.0001
41.0	0.8397	20.0	0.8241	0.0001	1.0000	0.0001
64.0	0.8494	30.0	0.8259	0.0001	0.9995	0.0001
		40.0	0.8256	0.0001	0.9989	0.0001
		50.0	0.8309	0.0001	0.9993	0.0001
		60.0	0.8332	0.0001	0.9992	0.0001

Physical Chemistry Chemical Physics

ARTICLE

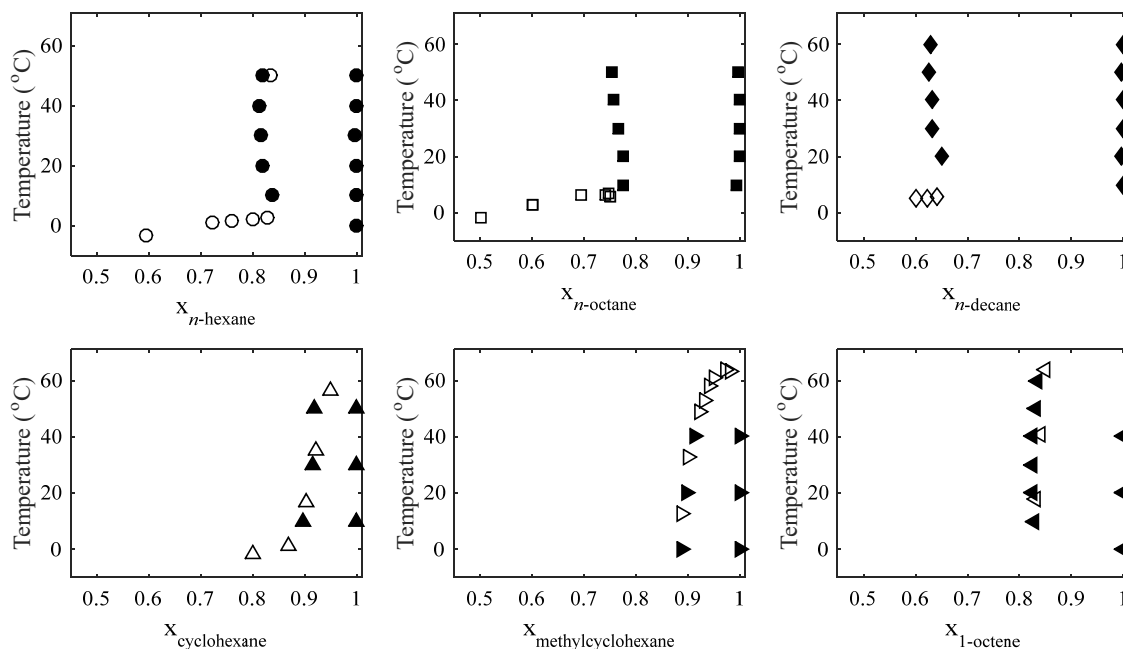


Figure 2 - T-x'-x'' diagrams (liquid/liquid equilibrium phase diagrams) for [oleyl-mim][NTf₂] with *n*-hexane, *n*-octane, *n*-decane, cyclohexane, methylcyclohexane and 1-octene. Open symbols are cloud point data and filled symbols are gravimetric data.

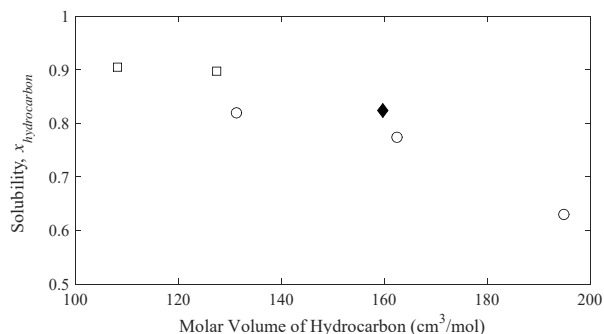


Figure 3 - Solubility of hydrocarbons in [oleyl-mim][NTf₂] at 25°C as a function of the hydrocarbon's molar volume.⁴⁶ The *n*-alkanes, *n*-hexane, *n*-octane and *n*-decane are shown as open circles (o) with molar volume increasing in the order listed. The cycloalkanes are shown as open squares (□) with molar volume increasing in the order listed. 1-Octene is shown as a solid diamond (◆).

the degree of distortion that could occur before the long range polar structure was completely lost. This would result in a sharp solubility limit with temperature, as observed in this work, with a significant temperature increase required to overcome the

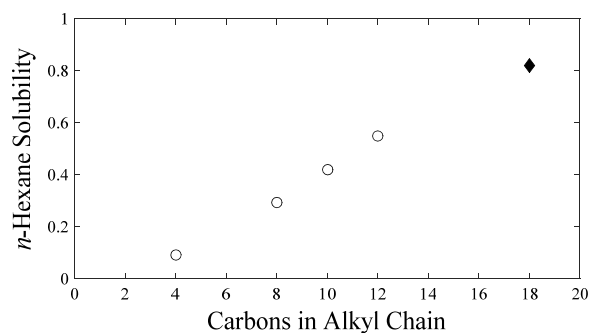


Figure 4 - Solubility of *n*-hexane at 25°C in 1-alkyl-3-methylimidazolium bistriflimide salts. The open circles (o) are literature data for saturated chains.⁴⁷ The filled diamond (◆) represents the value for the 18 carbon appended [oleyl-mim][NTf₂].

energy penalty of restructuring the polar sub-phase. This is consistent with the explanation of the solubility "wall" as presented above. Furthermore, analysis of the shapes of the nonpolar sub-phases⁶⁶ indicated that as the alkyl chain length increased, the nonpolar sub-phases transitioned from more

prolate (elongated, which might better accommodate extended chains) to oblate (more oval, which might better accommodate cyclic species of a similar size.) This observation may provide a molecular level reason, in addition to the volumetric arguments presented above, why the cyclic alkanes are more soluble than their straight chain analogues.

3.2. COSMO-RS Modelling

The results from the COSMO-RS model are shown in **Figure 5** for the hydrocarbons discussed above with the lipidic ionic liquid and are plotted along with the experimental data shown previously. The COSMO-RS model accurately captures the qualitative behavior of the six systems and reproduces several of the trends described above. Specifically, the COSMO-RS model predicts: the decreasing solubility of the *n*-alkanes with increasing molar volume (chain length), higher solubilities for the cyclohexane and methylcyclohexane than for the *n*-alkanes, and higher solubility for 1-octene than for its saturated analogue. Additionally, the model accurately predicts that the ionic liquid will have a very low solubility in the alkane, even though alkane solubility in the ionic liquid is high. Furthermore, the model predicts an upper critical solution temperature for the cyclic compounds in the same range as that observed experimentally. These observations are consistent with previous studies that have established the qualitative nature of COSMO-RS predictions for ionic liquid/hydrocarbon binary⁷⁶ and ternary equilibria.⁷⁷

The model is less accurate when predicting the steep temperature increase with solubility observed experimentally, explained above as a volumetric saturation effect. As described above, this phenomena may be due to the nano-segregated nature of this class of ionic liquid, which may not be fully captured by the COSMO-RS model. Additionally, the low temperature behaviour (below about 10°C) is not reproduced; again, this may be a gelling effect commonly seen in ionic liquids at low temperature and not well predicted by the model. Though it fails to quantitatively predict the liquid/liquid equilibria of these systems, the results agree qualitatively and suggest that such calculations are suitable as a tool for screening purposes to proceed synthesis/measurement or molecular dynamic simulations for similar systems.

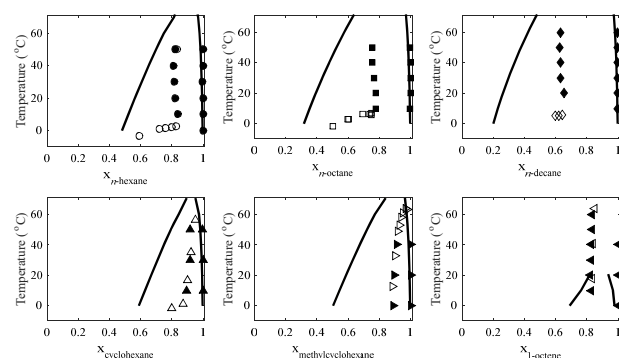


Figure 5 – COSMO-RS results (solid lines) for the miscibility gap (binodal) for [oleyl-mim][NTf₂] with *n*-hexane, *n*-octane, *n*-decane, cyclohexane, methylcyclohexane and 1-octene. Open symbols are cloud point data and filled symbols are gravimetric data.

4. Conclusions

Although ionic liquids are polar in nature due to their constituent ions, the structures of the ions can be altered to increase the nonpolar content, and thus increase the solubility of nonpolar solutes. Species with very long alkenyl appendages resemble natural lipids, and, like natural lipids, employ mid-chain unsaturations to lower melting points relative to saturated analogues. In this work, the solubilities of several nonpolar solutes are examined as functions of temperature for the lipidic ionic liquid [oleyl-mim][NTf₂]. Liquid-liquid equilibria consistent with upper critical solution behavior is observed, along with several trends related to the size and polarity of the solute. For *n*-alkanes, the solubility decreased with increasing molar volume; a similar trend was observed with cycloalkanes. Also, unsaturated 1-octene was slightly more soluble than saturated *n*-octane. This work demonstrates the highest solubility for *n*-alkanes in an ionic liquid at ambient conditions reported to date.

Interestingly, all of the solutes exhibited a very steep portion of the liquid-liquid equilibrium curve where the solubility became somewhat unaffected by temperature increases. This is potentially due to the solute being solely dissolved in the nonpolar region of the ionic liquid, until that region can no longer swell without disrupting the polar nano-domains. This could create a relatively uniform solubility limit, unaffected by temperature, requiring the breaking of polar/coulombic forces which necessitates higher temperatures, and is consistent with recent pure component molecular dynamics simulations of how the polar domain distorts as additional nonpolar content is added to the ionic liquid. The presence of this solubility limit “wall” and the solubility differences based on size/shape indicate that ionic liquids with similar properties may be synthesized to maximize these effects to enhance separations of nonpolar species. Molecular dynamic simulations of these systems may provide additional valuable insights into the origin of this behavior and provide direction into structure property relationship that could be exploited for effective separations. Furthermore, it was observed that a nearly pure hydrocarbon phase was in equilibrium with the ionic liquid/hydrocarbon phase which was 60-90% hydrocarbon. This is very significant because the ionic liquid is not significantly soluble in the hydrocarbon phase even though the ionic liquid dissolves a considerable amount of the hydrocarbon. Thus, for industrial liquid-liquid separations processes, the ionic liquid would not be stripped by the bulk hydrocarbon phase and lost in the process.

Acknowledgements

This material is based upon work supported by the National Science Foundation under Grant Number 1133101.

References

1. A. Carпов, *Cellul. Chem. Technol.*, 2005, **39**, 158-159.
2. N. V. Plechkova and K. R. Seddon, *Chem. Soc. Rev.*, 2008, **37**, 123-150.

3. J. H. Davis, Jr., *Chemistry Letters*, 2004, **33**, 1072-1077.
4. M. J. Earle and K. R. Seddon, *Pure Appl. Chem.*, 2000, **72**, 1391-1398.
5. J. L. Anderson, J. L. Anthony, J. F. Brennecke and E. J. Maginn, *Ionic Liquids in Synthesis (2nd Edition)*, 2008, **1**, 103-129.
6. J. L. Anderson, J. K. Dixon, E. J. Maginn and J. F. Brennecke, *J. Phys. Chem. B*, 2006, **110**, 15059-15062.
7. J. E. Bara, T. K. Carlisle, C. J. Gabriel, D. Camper, A. Finotello, D. L. Gin and R. D. Noble, *Industrial & Engineering Chemistry Research*, 2009, **48**, 2739-2751.
8. J. F. Brennecke, J. L. Anthony and E. J. Maginn, *Ionic Liquids in Synthesis*, 2003, 81-93.
9. M. B. Shiflett, A. M. S. Niehaus and A. Yokozeki, *The Journal of Physical Chemistry B*, 2011, **115**, 3478-3487.
10. J. H. Davis, Jr., US Patent # 2008-US59099-2008122030, US20080293978A1, 2008.
11. A. Arce, M. J. Earle, H. Rodriguez and K. R. Seddon, *Green Chem.*, 2007, **9**, 70-74.
12. U. Domanska, E. V. Lukoshko and M. Krolikowski, *J. Chem. Thermodyn.*, 2013, **61**, 126-131.
13. U. Domanska, A. Pobudkowska and F. Eckert, *Green Chem.*, 2006, **8**, 268-276.
14. E. Gomez, I. Dominguez, B. Gonzalez and A. Dominguez, *J. Chem. Eng. Data*, 2010, **55**, 5169-5175.
15. M. Larriba, P. Navarro, J. Garcia and F. Rodriguez, *J. Chem. Eng. Data*, 2014, **59**, 1692-1699.
16. M. Martinez-Reina, E. Amado-Gonzalez and Y. M. Munoz-Munoz, *Bull. Chem. Soc. Jpn.*, 2012, **85**, 1138-1144.
17. M. M. Reina, E. A. Gonzalez and Y. M. M. Munoz, *Rev. Colomb. Quim.*, 2012, **41**, 89-107.
18. C. Bidart, R. Jimenez, C. Carlesi, M. Flores and A. Berg, *Chemical Engineering Journal (Amsterdam, Netherlands)*, 2011, **175**, 388-395.
19. C. Chiappe and D. Pieraccini, *Journal of Physical Organic Chemistry*, 2005, **18**, 275-297.
20. J. P. Hallett and T. Welton, *Chemical Reviews*, 2011, **111**, 3508-3576.
21. J. R. Harjani, P. U. Naik, S. J. Nara and M. M. Salunkhe, *Curr. Org. Synth.*, 2007, **4**, 354-369.
22. P. S. Schulz, *Phosphorus Ligands Asymmetric Catal.*, 2008, **3**, 967-984.
23. F. Van Rantwijk and R. A. Sheldon, *Chemical Reviews (Washington, DC, United States)*, 2007, **107**, 2757-2785.
24. T. Welton and P. J. Smith, *Adv. Organomet. Chem.*, 2004, **51**, 251-284.
25. A. Heintz, D. V. Kulikov and S. P. Verevkin, *J. Chem. Eng. Data*, 2002, **47**, 894-899.
26. A. Heintz, S. P. Verevkin and D. Ondo, *J. Chem. Eng. Data*, 2006, **51**, 434-437.
27. J. P. Hallett and T. Welton, *ECS Transactions*, 2009, **16**, 33-38.
28. C. Wakai, A. Oleinikova, M. Ott and H. Weingärtner, *The Journal of Physical Chemistry B*, 2005, **109**, 17028-17030.
29. R. Hayes, G. G. Warr and R. Atkin, *Chemical Reviews*, 2015, **115**, 6357-6426.
30. U. Domańska and A. Marciniak, *Journal of Chemical & Engineering Data*, 2003, **48**, 451-456.
31. U. Domańska and A. Marciniak, *The Journal of Chemical Thermodynamics*, 2005, **37**, 577-585.
32. E. Torralba-Calleja, J. Skinner and D. Gutierrez-Tauste, *J. Chem.*, 2013, DOI: 10.1155/2013/473584, 473584/473581-473584/473517, 473517 pp.
33. Z. Lei, C. Dai and B. Chen, *Chemical Reviews (Washington, DC, United States)*, 2014, **114**, 1289-1326.
34. L. A. Blanchard and J. F. Brennecke, *Industrial & Engineering Chemistry Research*, 2001, **40**, 287-292.
35. X. Liu, W. Afzal, M. He and J. M. Prausnitz, *AIChE J.*, 2014, **60**, 2607-2612.
36. X. Liu, W. Afzal and J. M. Prausnitz, *Ind. Eng. Chem. Res.*, 2013, **52**, 14975-14978.
37. X. Liu, W. Afzal, G. Yu, M. He and J. M. Prausnitz, *J. Phys. Chem. B*, 2013, **117**, 10534-10539.
38. X. Liu, E. Ruiz, W. Afzal, V. Ferro, J. Palomar and J. M. Prausnitz, *Ind. Eng. Chem. Res.*, 2014, **53**, 363-368.
39. J. H. Davis, Jr., presented in part at the International Symposium on Ionic Liquids and Life Science, Keio University, Yokohama, Japan, August 11-12, 2007.
40. A. Mirjafari, S. M. Murray, R. A. O'Brien, A. C. Stenson, K. N. West and J. H. Davis, *Chem. Commun. (Cambridge, U. K.)*, 2012, **48**, 7522-7524.
41. S. M. Murray, R. A. O'Brien, K. M. Mattson, C. Ceccarelli, R. E. Sykora, K. N. West and J. H. Davis, Jr., *Angew. Chem., Int. Ed.*, 2010, **49**, 2755-2758.
42. S. M. Murray, T. K. Zimlich, A. Mirjafari, R. A. O'Brien, J. H. Davis, Jr. and K. N. West, *J. Chem. Eng. Data*, 2013, **58**, 1516-1522.
43. I. Lopez-Martin, E. Burello, P. N. Davey, K. R. Seddon and G. Rothenberg, *ChemPhysChem*, 2007, **8**, 690-695.
44. S. V. Dzyuba and R. A. Bartsch, *ChemPhysChem*, 2002, **3**, 161-166.
45. A. E. Bradley, C. Hardacre, J. D. Holbrey, S. Johnston, S. E. J. McMath and M. Nieuwenhuyzen, *Chemistry of Materials*, 2002, **14**, 629-635.
46. J. D. Holbrey and K. R. Seddon, *Journal of the Chemical Society, Dalton Transactions: Inorganic Chemistry*, 1999, 2133-2140.
47. C. M. Gordon, J. D. Holbrey, A. R. Kennedy and K. R. Seddon, *Journal of Materials Chemistry*, 1998, **8**, 2627-2636.
48. M.-L. Kwan, A. Mirjafari, J. R. McCabe, R. A. O'Brien, D. F. I. V. Essi, L. Baum, K. N. West and J. H. Davis, Jr., *Tetrahedron Lett.*, 2013, **54**, 12-14.
49. R. A. O'Brien, A. Mirjafari, K. M. Mattson, S. M. Murray, N. Mobarrez, E. A. Salter, A. Wierzbicki, J. H. Davis and K. N. West, *J. Phys. Chem. B*, 2014, **118**, 10232-10239.
50. A. Mirjafari, R. A. O'Brien, K. N. West and J. H. Davis, Jr., *Chem. - Eur. J.*, 2014, **20**, 7576-7580.
51. B. D. Green, R. A. O'Brien, J. H. Davis and K. N. West, *Ind. Eng. Chem. Res.*, 2015, **54**, 5165-5171.
52. A. Heintz, L. M. Casas, I. A. Nesterov, V. N. Emel'yanenko and S. P. Verevkin, *J. Chem. Eng. Data*, 2005, **50**, 1510-1514.
53. A. Heintz and S. P. Verevkin, *J. Chem. Eng. Data*, 2005, **50**, 1515-1519.
54. M. A. R. Martins, J. A. P. Coutinho, S. P. Pinho and U. Domanska, *J. Chem. Thermodyn.*, 2015, **91**, 194-203.
55. A. Marciniak, *Fluid Phase Equilibria*, 2010, **294**, 213-233.
56. S. Corderi, N. Calvar, E. Gomez and A. Dominguez, *Fluid Phase Equilib.*, 2012, **315**, 46-52.
57. S. Corderi, N. Calvar, E. Gomez and A. Dominguez, *J. Chem. Thermodyn.*, 2014, **76**, 79-86.
58. S. Corderi, E. J. Gonzalez, N. Calvar and A. Dominguez, *J. Chem. Thermodyn.*, 2012, **53**, 60-66.
59. J. Garcia, S. Garcia, J. S. Torrecilla and F. Rodriguez, *Fluid Phase Equilib.*, 2011, **301**, 62-66.
60. M. R. Heidari, B. Mokhtarani, N. Seghatoleslami, A. Sharifi and M. Mirzaei, *J. Chem. Thermodyn.*, 2012, **54**, 310-315.
61. J. N. A. Canongia Lopes and A. A. H. Padua, *J. Phys. Chem. B*, 2006, **110**, 3330-3335.
62. J. K. Shah and E. J. Maginn, *Fluid Phase Equilib.*, 2010, **294**, 197-205.
63. A. Triolo, O. Russina, H.-J. Bleif and C. E. Di, *J Phys Chem B*, 2007, **111**, 4641-4644.
64. Y. Wang and G. A. Voth, *Journal of the American Chemical Society*, 2005, **127**, 12192-12193.
65. S. M. Urahata and M. C. C. Ribeiro, *The Journal of Chemical Physics*, 2004, **120**, 1855-1863.

66. K. Shimizu, C. E. S. Bernardes and J. N. Canongia Lopes, *The Journal of Physical Chemistry B*, 2014, **118**, 567-576.
67. M. Brehm, H. Weber, M. Thomas, O. Hollóczki and B. Kirchner, *ChemPhysChem*, 2015, **16**, 3271-3277.
68. S. M. Murray, T. K. Zimlich, A. Mirjafari, R. A. O'Brien, J. H. Davis and K. N. West, *Journal of Chemical & Engineering Data*, 2013, **58**, 1516-1522.
69. F. Eckert and A. Klamt, *AIChE J.*, 2002, **48**, 369-385.
70. F. Eckert and A. Klamt, *Journal*, 2013.
71. TURBOMOLE, V6.6; University of Karlsruhe and Forschungszentrum Karlsruhe GmbH: Karlsruhe, Germany, 2014.
72. *COSMOconfX, Version 3.0; COSMOlogic GmbH & Co. KG: Leverkusen, Germany*, 2014.
73. C. L. Yaws, *Journal*, 2003.
74. O. Hollóczki, Z. Kelemen, L. Könczöl, D. Szieberth, L. Nyulászi, A. Stark and B. Kirchner, *ChemPhysChem*, 2013, **14**, 315-320.
75. A. Arce, M. J. Earle, H. Rodríguez and K. R. Seddon, *The Journal of Physical Chemistry B*, 2007, **111**, 4732-4736.
76. A. R. Ferreira, M. G. Freire, J. C. Ribeiro, F. M. Lopes, J. G. Crespo and J. A. P. Coutinho, *Ind. Eng. Chem. Res.*, 2011, **50**, 5279-5294.
77. A. R. Ferreira, M. G. Freire, J. C. Ribeiro, F. M. Lopes, J. G. Crespo and J. A. P. Coutinho, *Ind. Eng. Chem. Res.*, 2012, **51**, 3483-3507.